Received: 26 January 2021 | Revised: 20 July 2021 | Accepted: 21 July 2021

DOI: 10.1111/ter.12554

RESEARCH ARTICLE

Terra Nova WILEY

Assessing the robustness of carbonate-associated sulfate during hydrothermal dolomitization of the Latemar platform, Italy

Simon Lukas Schurr[1] | **Harald Strauss**[1] | **Mathias Mueller**[2] | **Adrian Immenhauser**[2,3]

[1]Institut für Geologie und Paläontologie, Westfälische-Wilhelms-Universität Münster, Münster, Germany

[2]Institute of Geology, Mineralogy and Geophysics, Ruhr-University Bochum, Bochum, Germany

[3]Fraunhofer IEG (Institution for Energy Infrastructures and Geothermal Systems), Bochum, Germany

Correspondence
Simon Lukas Schurr, Institut für Geologie und Paläontologie, Westfälische-Wilhelms-Universität Münster, Corrensstr. 24, 48149 Münster, Germany.
Email: simon-schurr@gmx.de

Funding information
Deutsche Forschungsgemeinschaft

Abstract

Carbonate-associated sulfate (CAS) is an important proxy for reconstructing marine sulfur cycling throughout Earth's history. In order to assess the impact of carbonate neomorphism on $\delta^{34}S_{CAS}$ data, a mineralogical-spatial transect from early diagenetic limestone into low-temperature hydrothermal dolostone was analyzed in the middle Triassic Latemar platform interior, northern Italy. This study addresses the yet unconstrained question whether hydrothermal dolostone preserves a marine $\delta^{34}S_{CAS}$ signature and, hence, might represent an archive for past seawater sulfate. In this study, $\delta^{34}S_{CAS}$ values were measured in low-temperature hydrothermal dolostone and compared with data from their corresponding precursor limestone. Results shown here reveal that $\delta^{34}S_{CAS}$ values for dolostone and precursor limestone are indistinguishable. This points to a rock-buffered middle Triassic marine $\delta^{34}S$ signature not affected by hydrothermal alteration. Hence, hydrothermal dolostone represents, under favorable conditions, an archive for unraveling past marine sulfur cycling.

1 | INTRODUCTION

Carbonate-associated sulfate (CAS) has been used for reconstructing marine sulfur cycling throughout Earth's history (Bottrell & Newton, 2006; Gill et al., 2007; Kampschulte & Strauss, 2004). Carbonate-associated sulfate is sulfate bound in the crystal lattice of carbonate minerals as a replacement for the carbonate ion (Burdett et al., 1989; Takano, 1985). Sulfate incorporation into carbonate minerals occurs without a substantial sulfur isotope fractionation and the sulfate records the sulfur isotopic composition of the ambient fluid (seawater or pore fluid) during carbonate precipitation (Burdett et al., 1989; Kampschulte & Strauss, 2004; Lyons et al., 2004, but see also Barkan et al., 2020).

Throughout Earth's rock record, dolostones are widely distributed from the Precambrian to the Cretaceous (Given & Wilkinson, 1987; Warren, 2000). Nevertheless, the applicability of $\delta^{34}S_{CAS}$ values from dolostone as a proxy for ancient seawater sulfate has not been well constrained (Fichtner et al., 2017; Marenco et al., 2008). Sulfur isotope data for CAS in dolostone, however, can either provide important insights into the chemistry of dolomitizing fluids or, under favorable conditions, reflect the marine $\delta^{34}S$ signature of the precursor limestone. Previous studies interpreted $\delta^{34}S_{CAS}$ values from early diagenetic dolostone to reflect fluid mixing between marine and continental sulfate (Marenco et al., 2008). In addition, sulfur isotope data can indicate microbial sulfur cycling such as microbial sulfate hate reduction or microbial sulfide oxidation (Baldermann et al., 2015; Fichtner et al., 2017). The processes related to sulfur cycling during hydrothermal dolomitization and fluid-rock interaction (Jonas et al., 2015, 2017) are complex. Arguably, different sulfur sources are recorded as CAS in the host dolostone, thereby masking the original marine $\delta^{34}S_{CAS}$ signature.

Recent hydrothermal dolomitization experiments reveal a comparably fast (weeks) replacement of calcite by (calcian) dolomite via Mg-rich fluids at temperatures above 100°C (Gregg et al., 2015; Jonas

[Correction added on 18 September 2021, after first online publication: Projekt Deal funding statement has been added.]

et al., 2015; Montes-Hernandez et al., 2016). Based on a dissolution-precipitation mechanism, controlled by porosity and permeability, precursor Ca-carbonate minerals are dissolved and replaced by highest-Mg calcites and/or (calcian) dolomites (Jonas et al., 2015, 2017; Kaczmarek & Sibley, 2014; Putnis, 2009). Furthermore, detailed geochemical studies of partially dolomitized carbonate edifices (e.g., Latemar platform) reveal insights into the geochemical mechanisms of hydrothermal dolomitization on a broader scale (Jacquemyn et al., 2014; Mueller, 2020; Mueller et al., 2020). In such settings, early diagenetic marine isotope signatures were either reported to become altered by hydrothermal dolomitization or display a conservative behavior even at temperatures above 150°C (Jacquemyn et al., 2014; Mueller, 2020; Mueller et al., 2020; Swart, 2015). Clearly, these patterns strongly depend on the parameter studied (e.g. $^{87}Sr/^{86}Sr$, $\delta^{13}C$).

In this study, we focus on the cycling of sulfur during hydrothermal limestone-to-dolostone transitions in the middle Triassic Latemar platform, Italy. We aim to assess the robustness of marine $\delta^{34}S_{CAS}$ data in hydrothermal dolostone and its potential for reconstructing marine sulfur cycling.

Statement of significance

Carbonate-associated sulfate (CAS) is used for reconstructing marine sulfur cycling throughout Earth's history. The degree of preservation of marine sulfur isotope values during hydrothermal dolomitization of limestone archives is poorly constrained. We investigated spatial transects across precursor limestone and hydrothermal dolostone with respect to sulfur cycling during low-temperature hydrothermal alteration. Our results reveal that the sulfur isotopic composition of CAS archived in dolostone is preserved during hydrothermal dolomitization. The implication is that, under favorable conditions, this proxy preserves marine sulfate sulfur isotopic composition despite mineralogical change.

2 | GEOLOGICAL SETTING

The Latemar platform is a well-studied isolated carbonate buildup 5 km north of Predazzo, northern Italy (Figure 1) (Bosellini, 1984; Brack et al., 1996; Christ et al., 2012; Egenhoff et al., 1999; Goldhammer et al., 1993; Marangon et al., 2011; Preto et al., 2001, 2005; Zühlke et al., 2003). The platform was formed over a comparably short-time interval (<5 Ma) during the Anisian–Ladinian as based on $^{206}Pb/^{238}U$ ages and biostratigraphy (Brack et al., 1996; Mundil et al., 2003). Controlled by sea-level fluctuations, the platform interior is riddled with exposure horizons capping longer-term shallowing-upward cycles (Brack et al., 1996; Christ et al., 2012; Marangon et al., 2011; Preto et al., 2001; Zühlke et al., 2003).

During the late Ladinian (~238 Ma), the emplacement of the Predazzo intrusion took place some 5 km to the southwest of the Latemar platform (Mundil et al., 1996). Multiple mafic dikes crosscut the carbonate platform (Blendinger, 1985; Blomme et al., 2017; Jacquemyn et al., 2014; Wilson et al., 1990). The circulation of associated hydrothermal fluids, possibly representing altered Carnian seawater, leached the mafic dikes and Fe- and Mg-rich fluids ultimately triggered dolomitization of the Latemar precursor limestones at approximately 80°C (Blomme et al., 2017; Carmichael et al., 2008; Jacquemyn et al., 2014; Wilson et al., 1990). The resulting meter-scale limestone-dolostone alternations represent an ideal natural laboratory to test the research question posed here.

3 | METHODS

Forty-two samples (lime- and dolostone) were collected at different locations on the Latemar platform top and in the Valsorda valley (Figure 1). For the identification of potential sulfur sources in the hydrothermal fluid, seven magmatic dikes on the Latemar platform and four samples from the stratigraphically underlying Werfen Formation in the Passo Feudo and Valsorda valleys were taken (Table 1, Figure 1).

Weathered material was removed using a diamond saw and rocks were powdered using a tungsten carbide mill. Carbonate-associated sulfate was extracted following a sequential wet chemical procedure detailed in (Wotte et al., 2012). Both, water-soluble sulfate (WSS) as well as CAS was precipitated as $BaSO_4$ and contents determined gravimetrically. Sulfide minerals (e.g. pyrite) were extracted via chromium reduction following (Canfield et al., 1986) and precipitated as Ag_2S.

Sulfur isotopes were measured via EA-IRMS using a Flash-EA-IsoLink-CN elemental analyzer interfaced with a Thermo Scientific Delta V Advantage at the University of Muenster. All samples were calibrated to the V-CDT scale with IAEA standards (S-1, S-2, S-3 and NBS-127). The long-term external reproducibility was ≤0.5‰ (2 *SD*).

Oxygen isotopes were analyzed via TC/EA-IRMS (Thermo Finnigan high-temperature conversion elemental analyzer connected with a Thermo Scientific Delta V Plus) at the University of Muenster. Oxygen isotope data of sulfate were calibrated to the V-SMOW scale with IAEA standards (SO-5, SO-6 and NBS-127) and revealed a long-term external reproducibility ≤1.0‰ (2 *SD*).

4 | RESULTS

At the Latemar (sample location 1–5 at Figure 1), limestone is a light-grey, fine-grained, laminated wackestone, and peloidal-microbial boundstone. The limestones are crosscut by mafic dikes with a width of approximately 2 m (Figure 2). The mafic rocks of dikes are greyish and fine-crystalline in nature. Frequently, dikes define the contact between precursor limestone and hydrothermal dolostone. Dolomite bodies have different sizes between 1

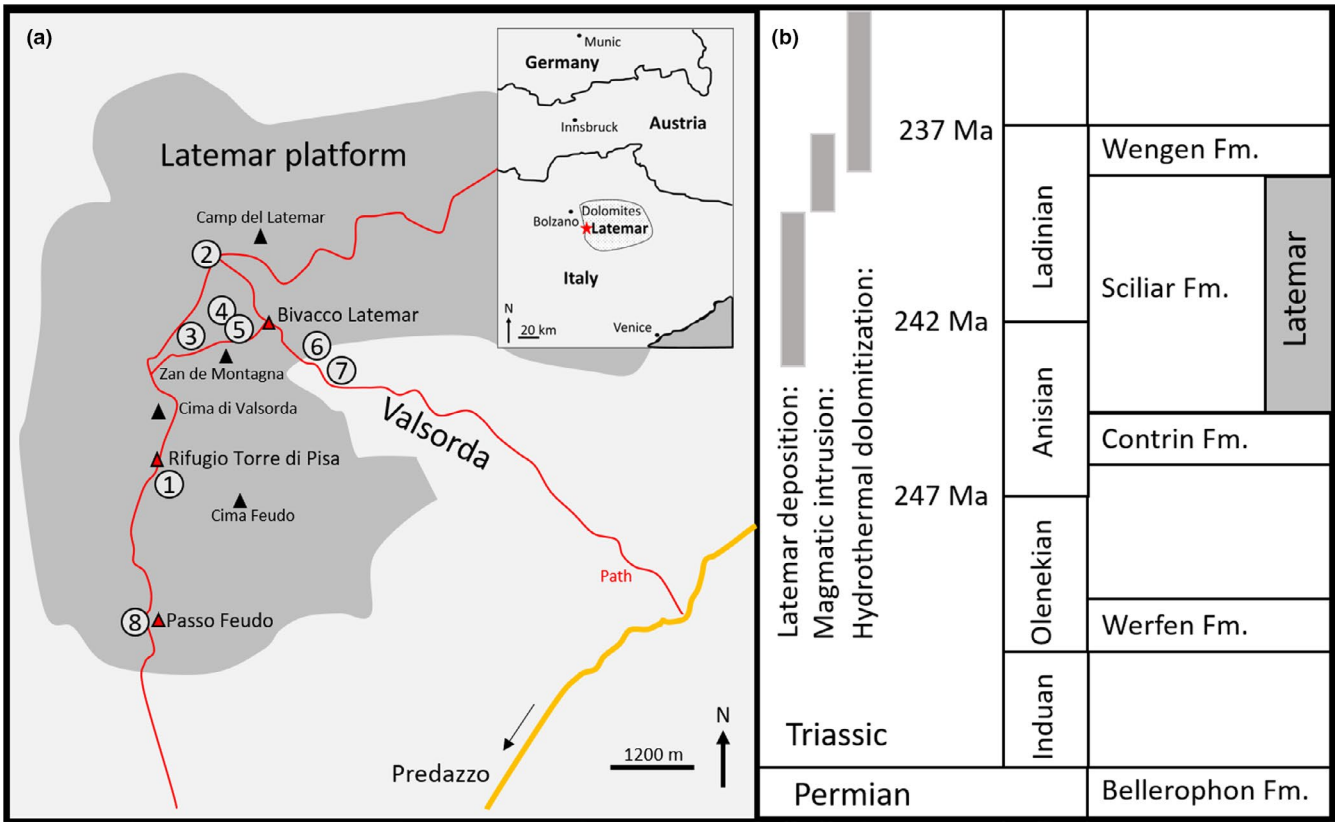

FIGURE 1 (a) Latemar platform situated in the Dolomites, 5 km north of Predazzo (northern Italy), number 1–8 present all sample locations (for geochemical data and coordinates of each location see Table 1). (b) Stratigraphic overview for the Latemar platform with regional formation names (Fm.) (Jacquemyn et al., 2014) and a simplified history of the Latemar platform deposition and its dolomitization (Blomme et al., 2017; Jacquemyn et al., 2014) [Colour figure can be viewed at wileyonlinelibrary.com]

and 10 m in dimension. Dolostones are tan brown with a fine-crystalline texture. Carbonates from the Werfen Formation are greyish, finely laminated microbial boundstones. Micrite is the dominant matrix material.

Chemical and isotopic data are summarized in Table 1. The CAS and WSS contents in the dolostone samples from the Latemar platform (avg. CAS = 240 ppm; avg. WSS = 110 ppm) are higher than those in limestone samples (avg. CAS = 120 ppm; avg. WSS = 20 ppm). By contrast, the sulfur and oxygen isotopic compositions of WSS in the dolostone (avg. $\delta^{34}S_{WSS}$ = 17.6‰; avg. $\delta^{18}O_{WSS}$ = 13.4‰) are near-identical compared with the precursor limestone (avg. $\delta^{34}S_{WSS}$ = 16.9‰; avg. $\delta^{18}O_{WSS}$ = 12.6‰). Likewise, dolostone samples have $\delta^{34}S_{CAS}$ around 20 ‰ and $\delta^{18}O_{CAS}$ values around 15‰ that are directly comparable when plotted against limestone samples (Figures 2 and 3).

Sulfide minerals in mafic dikes display an average $\delta^{34}S_{CRS}$ value of 1.0‰, whereas limestone and dolostone samples are devoid of sulfide minerals. Werfen Formation limestones exhibit the isotopically highest $\delta^{34}S_{CAS}$ values with 30.3‰ in the Valsorda valley and 39.9‰ at the Passo Feudo. Oxygen isotope data of CAS for samples from the Valsorda valley are on average 14‰ compared with a value of 19‰ for a sample taken at Passo Feudo. Limestone samples from the Werfen Formation show highly variable $\delta^{34}S_{CRS}$ values between −6.4‰ and 22.5‰.

5 | DISCUSSION AND INTERPRETATION

Water-soluble sulfate displays sulfur and oxygen isotope values (3‰ and 2‰, respectively) that are isotopically lower than the respective $\delta^{34}S_{CAS}$ data (Table 1). This points to sulfate (WSS fraction) originating from oxidized sulfide minerals (Wotte et al., 2012), emphasizing the importance of repeated leaching steps with 10% NaCl-solution prior to CAS extraction in order to obtain accurate $\delta^{34}S_{CAS}$ values.

Previous studies suggested that hydrothermal, Mg-rich fluids neomorphosed Latemar precursor limestone to dolostone (Jacquemyn et al., 2014). Consequently, a twofold higher CAS content in dolostone compared with limestone might suggest a net gain in sulfate from secondary sulfate sources during dolomitization (Figure 3).

Several scenarios, depending on the respective fluid source, are conceivable and lead to a replacement of the pristine CAS during dolomitization. These include (i) Carnian seawater, (ii) evaporite-rich sediments within the stratigraphically underlying succession, and (iii) the oxidation of magmatic sulfide minerals from cross-cutting dikes to sulfate.

In the marine environment, seawater sulfate represents an important sulfur source for hydrothermal fluids (Klugel et al., 2011). Jacquemyn et al. (2014) discussed hydrothermally heated Carnian

TABLE 1 Geochemical data for limestones, dolostones sampled at the Latemar platform. Locations 1–8 are shown in Figure 1. Absolute ages were determined by $^{206}Pb/^{238}U$ in zircons of ash layers from different altitudes at the Latemar platform (Zühlke et al., 2003)

Location	CAS (ppm)	$\delta^{34}S_{CAS}$ (‰) (V-CDT)	$\delta^{18}O_{CAS}$ (‰) (V-SMOW)	WSS (ppm)	$\delta^{34}S_{WSS}$ (‰) (V-CDT)	$\delta^{18}O_{WSS}$ (‰) (V-SMOW)	$\delta^{34}S_{CRS}$ (‰) (V-CDT)	
Upper sample location (2,670 m altitude)								
Age: 241.5 Ma (2,670 m altitude)								
Location 1: N46°21′39.0″; E11°33′35.3″								
R1-300817	1	19.3		45	16.7	13.6		Limestone
R2-300817	5	19.4		23	17.4			Limestone
R3-300817				24	17.1	13.0		Limestone
Location 1: N46°21′37.3″; E11°33′38.5″								
0-270817					17.2			Limestone
1-270817	15	19.8	13.4	37	17.7	12.9		Limestone
2-270817	7			10				Limestone
3-270817	30		13.7	117	16.8	13.0		Limestone
4-270817	178	19.7	14.9	161	17.4	12.9		Limestone
5-27-0817				20	16.9	12.3		Limestone
7-270817				43	18.0			Limestone
Location 2: N46°22′53.7″; E11°33′55.3″								
3B280817		19.2	12.6		17.1			Limestone
Middle sample location (2,600 m altitude)								
Age: 241.7 Ma (2,570 m altitude)								
Location 3: N46°22′00.8″; E11°33′39.8″								
S1	9	18.8		24	17.4	12.7		Limestone
S2				30	17.3	12.5		Limestone
S3							0.8	Dike
S4	390	20.5	15.5	430	18.1	13.0		Dolostone
S5							3.1	Dike
S6	21	20.6	14.2	161	20.2	12.9		Dolostone
S7	372	20.5	16.2	90	19.6	14.6		Dolostone
S8							−2.5	Dike
S9	578	20.5	16.0	421				Dolostone
S10	307	18.3	15.5	37	15.5	12.7		Dolostone
S11	210	20.5	14.8	33	15.6			Limestone
S12				22	12.5	12.5		Limestone
Location 4: N46°21′21.7″; E11°33′47.2″ to N46°22′22.3″; E11°33′58.2″								
F1	56	19.7		37	17.5			Limestone
F2	274	19.9	14.9	103				Dolostone
F3				58	17.1	9.7		Limestone
F4		19.0						Limestone
F5		17.4	11.0		16.6	10.3		Dolostone
F6		20.0			17.9	12.7		Limestone
F7	127	20.3	15.2	32	17.5	14.0		Dolostone
Lower sample location (2,350 m altitude)								
Age: 242.6 Ma (2,390 m altitude)								
Location 5: N46°22′22.7″; E11°33′58.2″								

(Continues)

TABLE 1 (Continued)

Location	CAS (ppm)	$\delta^{34}S_{CAS}$ (‰) (V-CDT)	$\delta^{18}O_{CAS}$ (‰) (V-SMOW)	WSS (ppm)	$\delta^{34}S_{WSS}$ (‰) (V-CDT)	$\delta^{18}O_{WSS}$ (‰) (V-SMOW)	$\delta^{34}S_{CRS}$ (‰) (V-CDT)	
01-300817	70	20.4	15.8	25				Limestone
03-300817	265	20.2	15.0	67	18.6	15.3		Dolostone
04-300817	358	20.5	17.0	7				Dolostone
05-300817	95	20.9	15.4	76	18.7	14.8		Dolostone
06-300817	59	20.4	14.3	11				Limestone
08-300817	460	19.9	15.8	26	18.6	14.7		Limestone
9-300817	125	19.9		194	18.6			Dolostone
Location 6: N46°22′36.7″; E11°34′55.9″								
DOL-1	285	20.8	15.6	36	19.0	14.9		Dolostone
M (L)	12	23.4	20.8	13	16.3	10.6		Limestone
DIKE 1 CRS							2.3	Dike
DIKE 2 CRS							2.4	Dike
DOL-2				14	12.6	11.5		Dolostone
Y1-DOL	6	20.8	16.3	6	16.7			Dolostone
Y-2-LIM				4	14.8			Limestone
Y-3-DOL	138	20.7	15.9	31				Dolostone
Y 4 CRS							0.3	Dike
Y5 CAS	173	19.2	15.5	14				Limestone
Y6 CAS	514	20.6	15.7	37				Limestone
Location 7: N46°22′34.7″; E11°34′53.8″								
P-1 CAS	1,120	30.4	14.2	140			−6.4	Limestone
P-2-Dike							0.4	Dike
P-3 CAS	1,162	30.1	14.3	195			1.6	Limestone
Werfen Fm.								
Location 8: N46°20′48.2″; E11°33′29.3″								
1-310817	460	39.9	19.2	83	22.4	10.4	22.5	Limestone

seawater as parent fluids for the dolomitization of the Latemar platform. Based on $\delta^{34}S$ measurements of Carnian evaporitic anhydrite, Carnian seawater is characterized by a $\delta^{34}S$ value around 16‰ (Bernasconi et al., 2017; Schroll & Rantitsch, 2005). Sulfur isotope values of CAS for dolostone samples display an average of 20.1‰ that is, however, substantially different from the Carnian seawater value (Figure 3). Consequently, and irrespective of an estimated marine sulfate concentration of ≥10 mM sulfate (Bernasconi et al., 2017), Carnian seawater is considered unlikely as the source of sulfur.

Dissolved sulfate in hydrothermal fluids causing the dolomitization of the Latemar platform might be derived from evaporitic sulfates from the stratigraphic succession underneath the Latemar edifice. The evaporite-rich Bellerophon Formation exhibits $\delta^{34}S$ values between 10.8‰ and 18.8‰ (Bernasconi et al., 2017; Newton et al., 2004), i.e. values that are decidedly lower than the $\delta^{34}S$ data obtained for lime- and dolostone samples at the Latemar (Figure 3). Moreover, $\delta^{18}O_{CAS}$ values for Latemar platform dolostone oscillate around an average of 15.3‰ and hence are slightly lower than the respective values for evaporitic Bellerophon sulfates (avg. = 17.1‰; Newton et al., 2004). Considering the differences in Bellerophon sulfate sulfur and oxygen isotope data, an evaporitic source during hydrothermal dolomitization of the Latemar platform is ruled out.

Sulfate-rich Werfen Formation sedimentary rocks are stratigraphically situated beneath the Latemar platform and represent another possible sulfate source. However, $\delta^{34}S_{CAS}$ values of 30.3‰ and 39.9‰ for limestones of the lower Triassic Werfen Formation are significantly enriched in ^{34}S compared with $\delta^{34}S_{CAS}$ values for the Latemar limestone and dolostone samples. The strongly ^{34}S-enriched sulfur isotopic composition reflects microbial sulfate reduction during early diagenesis (Bernasconi et al., 2017; Newton et al., 2004). Sulfide minerals of the Werfen Formation show a wide range in $\delta^{34}S$ (−6.4‰ to 22.5‰). These sulfur isotope values reflect pyrite precipitation from progressively ^{34}S enriched porewater sulfide resulting from microbial sulfate reduction in a sulfate-poor marine sediment (Fike et al., 2015). In conclusion, sulfate mobilized from different carbonates and evaporites from the Bellerophon

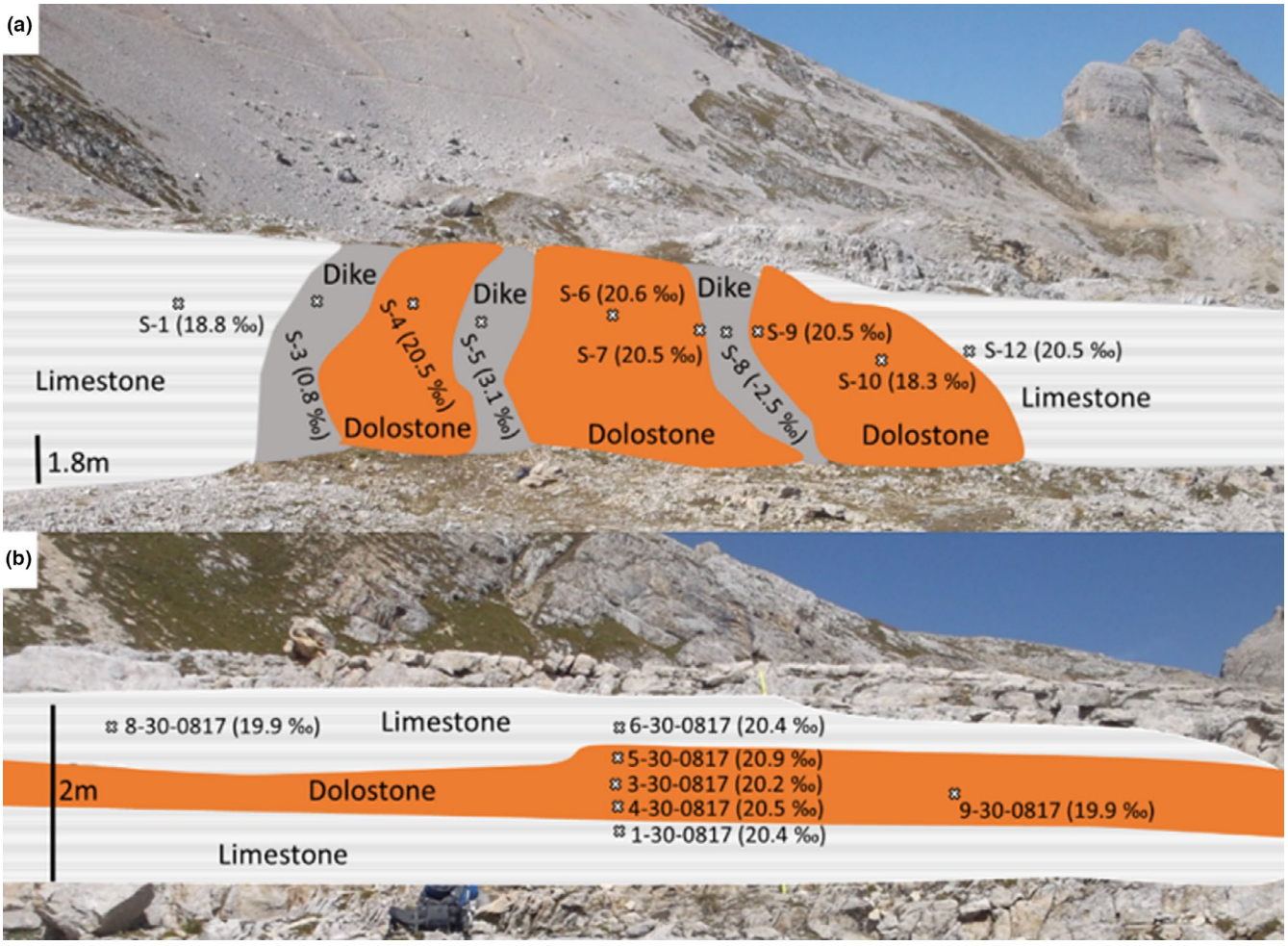

FIGURE 2 Locations 3 (a) and 5 (b) with $\delta^{34}S$ data for carbonate-associated sulfate and magmatic sulfide minerals of the dikes ($\delta^{34}S_{CRS}$) [Colour figure can be viewed at wileyonlinelibrary.com]

Formation and the Werfen Formation (Figure 3) are further excluded as sources for sulfate in the dolomitizing fluid.

A last possible source of sulfate in the hydrothermal fluids is the oxidation of sulfide minerals from the mafic dikes (avg. $\delta^{34}S = 1.0‰$) displaying a magmatic sulfur source (Sakai et al., 1984). Hydrothermal fluids interacted with mafic dikes, thereby oxidizing magmatic sulfides to sulfate. The resulting sulfate is expected to exhibit a sulfur isotopic composition that is similar to the magmatic sulfide with only a small sulfur isotope fractionation (ca. −0.7‰; Balci et al., 2007) associated with abiotic sulfide oxidation. If sulfate resulted from oxidized magmatic sulfide minerals, oxidized sulfate would represent an important source of sulfate in the dolomitizing fluid. Consequently, $\delta^{34}S_{CAS}$ values of dolostone are expected to display a significantly lower sulfur isotope signature compared with the precursor limestone.

The average CAS content in dolostone samples is two-fold higher compared with that in limestone samples, but respective $\delta^{34}S$ and $\delta^{18}O$ values are indistinguishable. This result is in clear contrast to previous work (Marenco et al., 2008), reporting an eight-fold higher CAS content for early diagenetic (calcian) dolostone. Corresponding $\delta^{34}S_{CAS}$ values, however, were up to 5‰ lower than those in the precursor limestone and were best assigned to a continentally-derived fluid source during dolomitization. Moreover, no correlation between the CAS and the Mg content of the dolostone in the Latemar platform is discernible, again much in contrast to previous studies, which reported a correlation between a higher Mg-content in Mg-carbonates and a lower CAS content (Baldermann et al., 2015; Fichtner et al., 2017). These authors reasoned that a higher degree of crystallographic order caused a reduction in space in the crystal lattice too small for the relatively large sulfate ion. At present, the combination of an elevated CAS content in dolostone samples from the Latemar and the directly comparable sulfur isotopic composition ($\delta^{34}S_{CAS}$) in precursor limestone remains enigmatic.

Thus far, $\delta^{34}S_{CAS}$ values determined for dolostone and precursor limestone at the Latemar platform are indistinguishable and no secondary sulfate sources were identified that altered or even replaced the marine $\delta^{34}S_{CAS}$ signature during hydrothermal dolomitization (Figure 3). In the light of this observation, CAS data also for hydrothermal dolostone at the Latemar are considered to reflect the isotopic composition of middle Triassic seawater sulfate. Consequently, $\delta^{34}S_{CAS}$ data obtained here for limestone, but also for

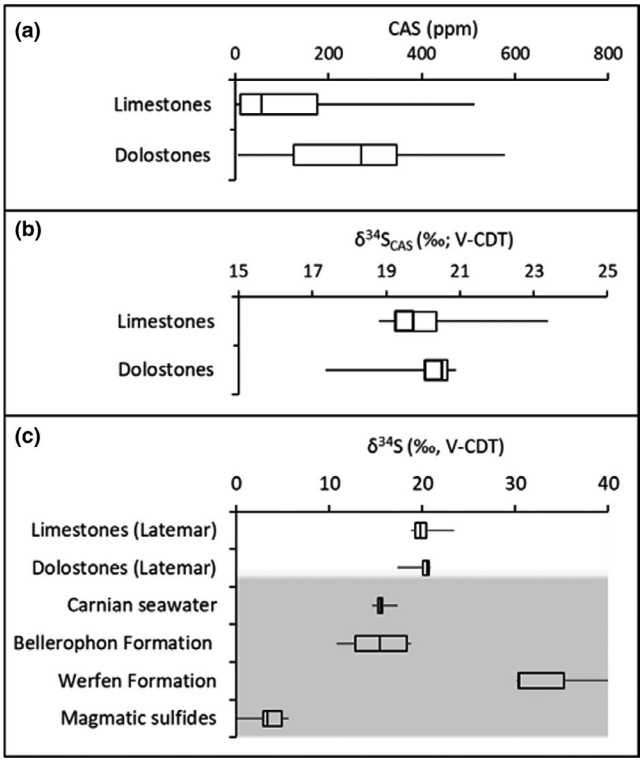

FIGURE 3 (a) Dolostones ($n = 14$, 1 *SD* = 260 ppm) reveal a higher carbonate-associated sulfate (CAS) content compared with limestones ($n = 15$, 1 *SD* = 260 ppm). (b) The average $\delta^{34}S_{CAS}$ value of 20.1‰ for dolostones ($n = 15$, 1 *SD* = 1.0‰), however, is indistinguishable to the average of 19.9‰ for limestones ($n = 16$, 1 *SD* = 1.0‰). (c) Sulfur isotope data for all CAS samples (limestones, $n = 15$, and dolostones, $n = 16$) of the Latemar platform combined with sulfur isotopes of Carnian seawater (anhydrite, $n = 165$, (Bernasconi et al., 2017), Bellerophon Formation (CAS, $n = 11$, Newton et al., 2004), Werfen Formation (CAS, $n = 3$, this study) and magmatic sulfide (CRS, $n = 7$, this study)

dolostone samples, provide insight into marine sulfur cycling during the Anisian–Ladinian stages (Figure 4).

6 | CONCLUSION

Sulfur isotope data for CAS from limestone and hydrothermal low-temperature dolostone from the middle Triassic Latemar platform, Italy, were assessed in order to constrain the robustness of $\delta^{34}S_{CAS}$ data in dolostone archives. Irrespective of significant fluid–rock interaction during hydrothermal dolomitization, no shift in dolostone $\delta^{34}S_{CAS}$ data due to diagenetic sulfur sources (Carnian seawater sulfate, sulfate-rich sediments, and oxidation of magmatic sulfide minerals) is found. This study documents a genuine rock-buffered diagenetic system that did not reset marine $\delta^{34}S_{CAS}$ values reflecting middle Triassic seawater sulfate. Evidence is presented that, under favorable conditions, the marine $\delta^{34}S_{CAS}$ signature remains well preserved during low-temperature hydrothermal alteration and dolomitization of marine limestone. This outcome is of significance

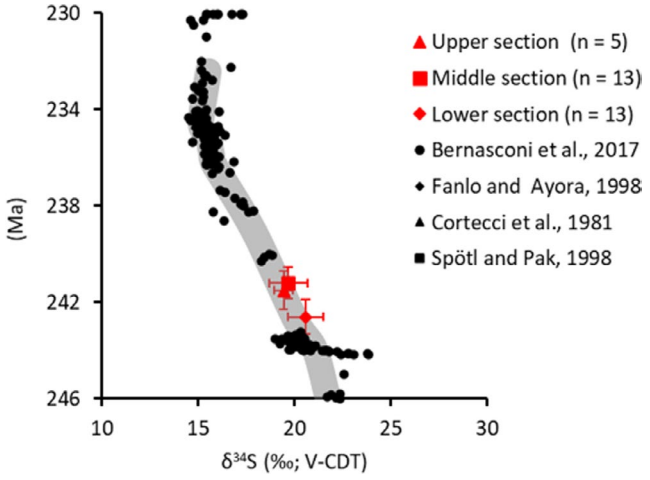

FIGURE 4 Sulfur isotope record for middle Triassic seawater sulfate with $\delta^{34}S_{CAS}$ data from the Latemar platform (divided into a lower, middle, and upper sample location) combined with $\delta^{34}S$ data for anhydrite (Bernasconi et al., 2017; Cortecci et al., 1981; Fanlo & Ayora, 1998; Spötl & Pak, 1996). Error bars show confidence levels of absolute ages (Zühlke et al., 2003) and 2 *SD* of $\delta^{34}S_{CAS}$ data [Colour figure can be viewed at wileyonlinelibrary.com]

for those concerned with deep-time carbonate archives often dominated by early marine or hydrothermal diagenetic dolostone.

ACKNOWLEDGEMENTS

This study was supported by the Deutsche Forschungsgemeinschaft in the DFG-project CHARON (1644-Phase II). We are grateful to the Gabrielli Family, the owners of the Rifugio Torre di Pisa, for the logistic help on the Latemar platform. We thank Artur Fugmann for the technical assistance and support in the lab. For discussions and helpful advices, we acknowledge Carl Jaquemyn and Vanessa Fichtner. Open Access funding enabled and organized by Projekt DEAL.

CONFLICT OF INTEREST

None.

DATA AVAILABILITY STATEMENT

The data that supports the findings of this study are available in the supplementary material of this article.

REFERENCES

Balci, N., Shanks, W. C., Mayer, B., & Mandernack, K. W. (2007). Oxygen and sulfur isotope systematics of sulfate produced by bacterial and abiotic oxidation of pyrite. *Geochimica Et Cosmochimica Acta*, *71*(15), 3796–3811. https://doi.org/10.1016/j.gca.2007.04.017

Baldermann, A., Deditius, A. P., Dietzel, M., Fichtner, V., Fischer, C., Hippler, D., Leis, A., Baldermann, C., Mavromatis, V., Stickler, C. P., & Strauss, H. (2015). The role of bacterial sulfate reduction during dolomite precipitation: Implications from Upper Jurassic platform carbonates. *Chemical Geology*, *412*, 1–14. https://doi.org/10.1016/j.chemgeo.2015.07.020

Barkan, Y., Paris, G., Webb, S. M., Adkins, J. F., & Halevy, I. (2020). Sulfur isotope fractionation between aqueous and carbonate-associated sulfate in abiotic calcite and aragonite. *Geochimica Et Cosmochimica Acta*, *280*, 317–339. https://doi.org/10.1016/j.gca.2020.03.022

Bernasconi, S. M., Meier, I., Wohlwend, S., Brack, P., Hochuli, P. A., Bläsi, H., Wortmann, U. G., & Ramseyer, K. (2017). An evaporite-based high-resolution sulfur isotope record of Late Permian and Triassic seawater sulfate. *Geochimica Et Cosmochimica Acta*, *204*, 331–349. https://doi.org/10.1016/j.gca.2017.01.047

Blendinger, W. (1985). Middle Triassic strike-slip tectonics and igneous activity of the Dolomites (Southern Alps). *Tectonophysics*, *113*(1–2), 105–121. https://doi.org/10.1016/0040-1951(85)90112-X

Blomme, K., Fowler, S. J., Bachaud, P., Nader, F. H., Michel, A., & Swennen, R. (2017). Ferroan dolomitization by seawater interaction with mafic igneous dikes and carbonate host rock at the Latemar Platform, Dolomites, Italy: Numerical modeling of spatial, temporal, and temperature data. *Geofluids*, *2017*, 1–14. https://doi.org/10.1155/2017/6590672

Bosellini, A. (1984). Progradation geometries of carbonate platforms: Examples from the Triassic of the Dolomites, northern Italy. *Sedimentology*, *31*(1), 1–24. https://doi.org/10.1111/j.1365-3091.1984.tb00720.x

Bottrell, S. H., & Newton, R. J. (2006). Reconstruction of changes in global sulfur cycling from marine sulfate isotopes. *Earth-Science Reviews*, *75*(1–4), 59–83. https://doi.org/10.1016/j.earscirev.2005.10.004

Brack, P., Mundil, R., Oberli, F., Meier, M., & Rieber, H. (1996). Biostratigraphic and radiometric age data question the Milankovitch characteristics of the Latemar cycles (Southern Alps, Italy). *Geology*, *24*(4), 371. https://doi.org/10.1130/0091-7613(1996)024<0371:BARADQ>2.3.CO;2

Burdett, J. W., Arthur, M. A., & Richardson, M. (1989). A Neogene seawater sulfur isotope age curve from calcareous pelagic microfossils. *Earth and Planetary Science Letters*, *94*(3), 189–198. https://doi.org/10.1016/0012-821X(89)90138-6

Canfield, D. E., Raiswell, R., Westrich, J. T., Reaves, C. M., & Berner, R. A. (1986). The use of chromium reduction in the analysis of reduced inorganic sulfur in sediments and shales. *Chemical Geology*, *54*, 149–155. https://doi.org/10.1016/0009-2541(86)90078-1

Carmichael, S. K., Ferry, J. M., & McDonough, W. F. (2008). Formation of replacement dolomite in the Latemar carbonate buildup, Dolomites, northern Italy: Part 1. Field relations, mineralogy, and geochemistry. *American Journal of Science*, *308*(7), 851–884. https://doi.org/10.2475/07.2008.03

Christ, N., Immenhauser, A., Amour, F., Mutti, M., Preston, R., Whitaker, F. F., Peterhänsel, A., Egenhoff, S. O., Dunn, P. A., & Agar, S. M. (2012). Triassic Latemar cycle tops — Subaerial exposure of platform carbonates under tropical arid climate. *Sedimentary Geology*, *265–266*, 1–29. https://doi.org/10.1016/j.sedgeo.2012.02.008

Cortecci, G., Reyes, E., Berti, G., & Casati, P. (1981). Sulfur and oxygen isotopes in Italian marine sulfates of Permian and Triassic ages. *Chemical Geology*, *34*(1), 65–79. https://doi.org/10.1016/0009-2541(81)90072-3. Retrieved from http://www.sciencedirect.com/science/article/pii/0009254181900723

Egenhoff, S. O., Peterhansel, A., Bechstadt, T., Zuhlke, R., & Grotsch, J. (1999). Facies architecture of an isolated carbonate platform: Tracing the cycles of the Latemar (Middle Triassic, northern Italy). *Sedimentology*, *46*(5), 893–912. https://doi.org/10.1046/j.1365-3091.1999.00258.x

Fanlo, I., & Ayora, C. (1998). The evolution of the Lorraine evaporite basin: Implications for the chemical and isotope composition of the Triassic ocean. *Chemical Geology*, *146*(3), 135–154. https://doi.org/10.1016/S0009-2541(98)00007-2

Fichtner, V., Strauss, H., Immenhauser, A., Buhl, D., Neuser, R. D., & Niedermayr, A. (2017). Diagenesis of carbonate associated sulfate. *Chemical Geology*, *463*, 61–75. https://doi.org/10.1016/j.chemgeo.2017.05.008

Fike, D. A., Bradley, A. S., & Rose, C. V. (2015). Rethinking the ancient sulfur cycle. *Annual Review of Earth and Planetary Sciences*, *43*(1), 593–622. https://doi.org/10.1146/annurev-earth-060313-054802

Gill, B. C., Lyons, T. W., & Saltzman, M. R. (2007). Parallel, high-resolution carbon and sulfur isotope records of the evolving Paleozoic marine sulfur reservoir. *Palaeogeography, Palaeoclimatology, Palaeoecology*, *256*(3–4), 156–173. https://doi.org/10.1016/j.palaeo.2007.02.030

Given, R. K., & Wilkinson, B. H. (1987). Dolomite abundance and stratigraphic age; constraints on rates and mechanisms of Phanerozoic dolostone formation. *Journal of Sedimentary Research*, *57*(6), 1068–1078. https://doi.org/10.1306/212F8CF1-2B24-11D7-8648000102C1865D

Goldhammer, R. K., Harris, M. T., Dunn, P. A., & Hardie, L. A. (1993). Sequence Stratigraphy and Systems Tract Development of the Latemar Platform, Middle Triassic of the Dolomites (Northern Italy). In R. G. Loucks & J. F. Sarg (Eds.), *Carbonate sequence stratigraphy* (pp. 353–387). American Association of Petroleum Geologists.

Gregg, J. M., Bish, D. L., Kaczmarek, S. E., & Machel, H. G. (2015). Mineralogy, nucleation and growth of dolomite in the laboratory and sedimentary environment: A review. *Sedimentology*, *62*(6), 1749–1769. https://doi.org/10.1111/sed.12202

Jacquemyn, C., El Desouky, H., Hunt, D., Casini, G., & Swennen, R. (2014). Dolomitization of the Latemar platform: Fluid flow and dolomite evolution. *Marine and Petroleum Geology*, *55*, 43–67. https://doi.org/10.1016/j.marpetgeo.2014.01.017

Jonas, L., Müller, T., Dohmen, R., Baumgartner, L., & Putlitz, B. (2015). Transport-controlled hydrothermal replacement of calcite by Mg-carbonates. *Geology*, *43*(9), 779–782. https://doi.org/10.1130/G36934.1

Jonas, L., Müller, T., Dohmen, R., Immenhauser, A., & Putlitz, B. (2017). Hydrothermal replacement of biogenic and abiogenic aragonite by Mg-carbonates – Relation between textural control on effective element fluxes and resulting carbonate phase. *Geochimica Et Cosmochimica Acta*, *196*, 289–306. https://doi.org/10.1016/j.gca.2016.09.034

Kaczmarek, S. E., & Sibley, D. F. (2014). Direct physical evidence of dolomite recrystallization. *Sedimentology*, *61*(6), 1862–1882. https://doi.org/10.1111/sed.12119

Kampschulte, A., & Strauss, H. (2004). The sulfur isotopic evolution of Phanerozoic seawater based on the analysis of structurally substituted sulfate in carbonates. *Chemical Geology*, *204*(3), 255–286. https://doi.org/10.1016/j.chemgeo.2003.11.013

Klugel, A., Hansteen, T. H., van den Bogaard, P., Strauss, H., & Hauff, F. (2011). Holocene fluid venting at an extinct Cretaceous seamount. *Canary Archipelago. Geochimica Et Cosmochimica Acta*, *39*(9), 855–858. https://doi.org/10.1130/G32006.1

Lyons, T. W., Walter, L. M., Gellatly, A. M., Martini, A. M., & Blake, R. E. (2004). Sites of anomalous organic remineralization in the carbonate sediments of South Florida, USA: The sulfur cycle and carbonate-associated sulfate. In J. P. Amend, K. J. Edwards, & T. W. Lyons (Eds.), *Sulfur biogeochemistry - past and present*, vol. *379*. Geological Society of America, p. 0.

Marangon, A., Gattolin, G., Della Porta, G., & Preto, N. (2011). The Latemar: A flat-topped, steep fronted platform dominated by microbialites and synsedimentary cements. *Sedimentary Geology*, *240*(3–4), 97–114. https://doi.org/10.1016/j.sedgeo.2011.09.001

Marenco, P. J., Corsetti, F. A., Kaufman, A. J., & Bottjer, D. J. (2008). Environmental and diagenetic variations in carbonate associated sulfate: An investigation of CAS in the Lower Triassic of the western USA. *Geochimica Et Cosmochimica Acta*, *72*(6), 1570–1582. https://doi.org/10.1016/j.gca.2007.10.033

Montes-Hernandez, G., Findling, N., & Renard, F. (2016). Dissolution-precipitation reactions controlling fast formation of dolomite under hydrothermal conditions. *Applied Geochemistry*, *73*, 169–177. https://doi.org/10.1016/j.apgeochem.2016.08.011

Mueller, M. (2020). *Assessing the reliability of dolostones as palaeoenvironmental archives*. Dissertation, Ruhr-Universität Bochum, Bochum, 261 pp.

Mueller, M., Igbokwe, O. A., Walter, B., Pederson, C. L., Riechelmann, S., Richter, D. K., Albert, R., Gerdes, A., Buhl, D., Neuser, R. D., Bertotti, G., & Immenhauser, A. (2020). Testing the preservation potential of early diagenetic dolomites as geochemical archives. *Sedimentology*, *67*(2), 849–881. https://doi.org/10.1111/sed.12664

Mundil, R., Brack, P., Meier, M., Rieber, H., & Oberli, F. (1996). High resolution U-Pb dating of Middle Triassic volcaniclastics: Time-scale calibration and verification of tuning parameters for carbonate sedimentation. *Earth and Planetary Science Letters*, *141*(1–4), 137–151. https://doi.org/10.1016/0012-821X(96)00057-X

Mundil, R., Zühlke, R., Bechstädt, T., Peterhänsel, A., Egenhoff, S. O., Oberli, F., Meier, M., Brack, P., & Rieber, H. (2003). Cyclicities in Triassic platform carbonates: Synchronizing radio-isotopic and orbital clocks. *Terra Nova*, *15*(2), 81–87. https://doi.org/10.1046/j.1365-3121.2003.00475.x

Newton, R. J., Pevitt, E. L., Wignall, P. B., & Bottrell, S. H. (2004). Large shifts in the isotopic composition of seawater sulphate across the Permo-Triassic boundary in northern Italy. *Earth and Planetary Science Letters*, *218*(3–4), 331–345. https://doi.org/10.1016/S0012-821X(03)00676-9

Preto, N., Hinnov, L. A., Hardie, L. A., & Harris, M. T. (2005). Sea level changes versus hydrothermal diagenesis: Origin of Triassic carbonate platform cycles in the Dolomites, Italy—Discussion. *Sedimentary Geology*, *178*(1–2), 135–139. https://doi.org/10.1016/j.sedgeo.2005.03.002

Preto, N., Hinnov, L. A., Hardie, L. A., & Zanche, V. D. (2001). Middle Triassic orbital signature recorded in the shallow-marine Latemar carbonate buildup (Dolomites, Italy). *Geology*, *29*(12), 1123. https://doi.org/10.1130/0091-7613(2001)029<1123:MTOSRI>2.0.CO;2

Putnis, A. (2009). Mineral replacement reactions. *Reviews in Mineralogy and Geochemistry*, *70*(1), 87–124. https://doi.org/10.2138/rmg.2009.70.3

Sakai, H., Marais, D. J. D., Ueda, A., & Moore, J. G. (1984). Concentrations and isotope ratios of carbon, nitrogen and sulfur in ocean-floor basalts. *Geochimica Et Cosmochimica Acta*, *48*(12), 2433–2441. https://doi.org/10.1016/0016-7037(84)90295-3

Schroll, E., & Rantitsch, G. (2005). Sulphur isotope patterns from the Bleiberg deposit (Eastern Alps) and their implications for genetically affiliated lead-zinc deposits. *Mineralogy and Petrology*, *84*(1–2), 1–18. https://doi.org/10.1007/s00710-004-0071-3

Spötl, C., & Pak, E. (1996). A strontium and sulfur isotopic study of Permo-Triassic evaporites in the Northern Calcareous Alps, Austria. *Chemical Geology*, *131*(1), 219–234. https://doi.org/10.1016/0009-2541(96)00017-4

Swart, P. K. (2015). The geochemistry of carbonate diagenesis: The past, present and future. *Sedimentology*, *62*(5), 1233–1304. https://doi.org/10.1111/sed.12205

Takano, B. (1985). Geochemical implications of sulfate in sedimentary carbonates. *Chemical Geology*, *49*(4), 393–403. https://doi.org/10.1016/0009-2541(85)90001-4

Warren, J. (2000). Dolomite: Occurrence, evolution and economically important associations. *Earth-Science Reviews*, *52*(1–3), 1–81. https://doi.org/10.1016/S0012-8252(00)00022-2

Wilson, E. N., Hardie, L. A., & Phillips, O. M. (1990). Dolomitization front geometry, fluid flow patterns, and the origin of massive dolomite; the Triassic Latemar buildup, northern Italy. *American Journal of Science*, *290*(7), 741–796. https://doi.org/10.2475/ajs.290.7.741

Wotte, T., Shields-Zhou, G. A., & Strauss, H. (2012). Carbonate-associated sulfate: Experimental comparisons of common extraction methods and recommendations toward a standard analytical protocol. *Chemical Geology*, *326–327*, 132–144. https://doi.org/10.1016/j.chemgeo.2012.07.020

Zühlke, R., Bechstadt, T., & Mundil, R. (2003). Sub-Milankovitch and Milankovitch forcing on a model Mesozoic carbonate platform - the Latemar (Middle Triassic, Italy). *Terra Nova*, *15*(2), 69–80. https://doi.org/10.1046/j.1365-3121.2003.00366.x

How to cite this article: Schurr, S. L., Strauss, H., Mueller, M., & Immenhauser, A. (2021). Assessing the robustness of carbonate-associated sulfate during hydrothermal dolomitization of the Latemar platform, Italy. *Terra Nova*, 33, 621–629. https://doi.org/10.1111/ter.12554